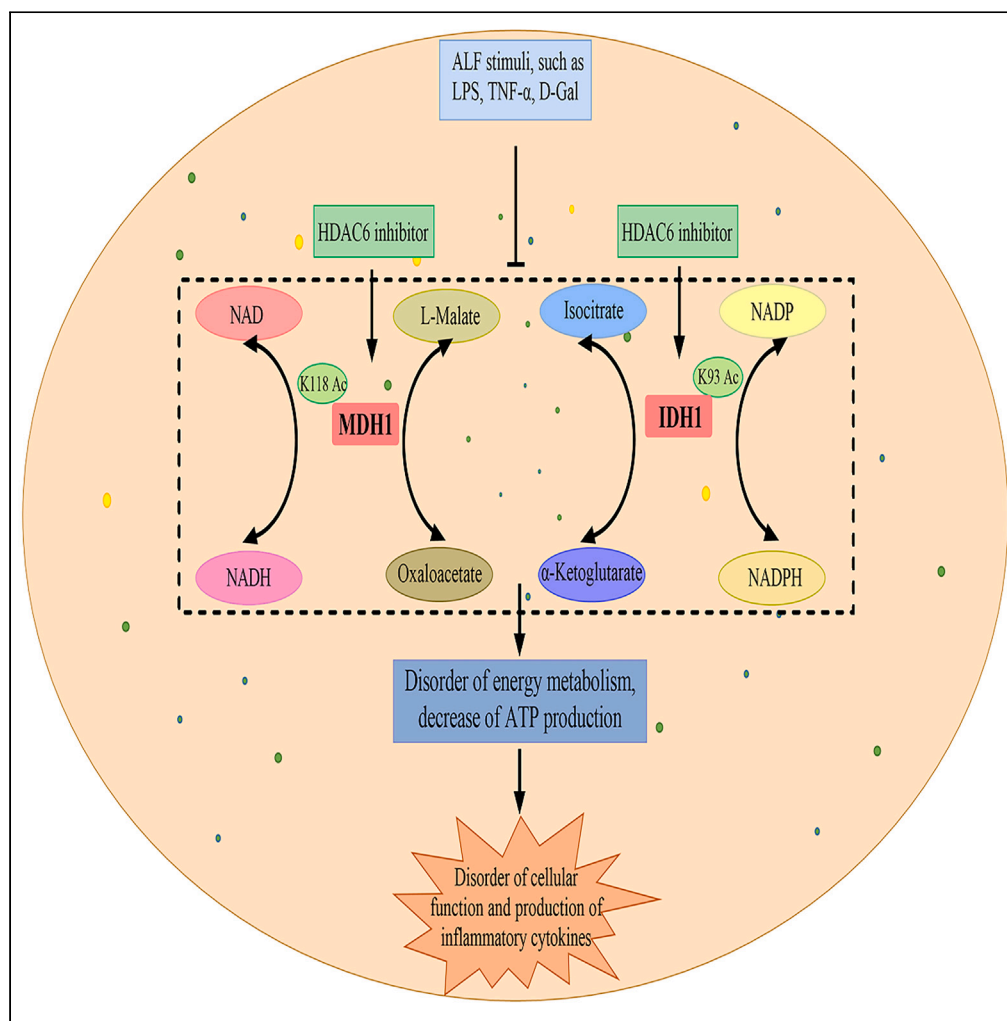


Article

The acetylation of MDH1 and IDH1 is associated with energy metabolism in acute liver failure



Chunxia Shi,
Yanqiong Zhang,
Qian Chen, ...,
Qingqi Zhang,
Wenbin Zhang,
Zuojiong Gong

zjgong@163.com

Highlights

Energy metabolism in the liver tissue of ALF patients was disordered

The HDAC inhibitor ACY1215 increased MDH1 and IDH1 expression and improved energy metabolism

ACY1215 rescued MDH1 and IDH1 expression after treatment with MDH1-siRNA and IDH1-siRNA

The acetylation of MDH1 K118 and IDH1 K93 sites is associated with energy metabolism in ALF

Shi et al., iScience 27, 109678
May 17, 2024 © 2024 The Authors. Published by Elsevier Inc.
<https://doi.org/10.1016/j.isci.2024.109678>

Article

The acetylation of MDH1 and IDH1 is associated with energy metabolism in acute liver failure

Chunxia Shi,^{1,4} Yanqiong Zhang,^{1,4} Qian Chen,² Yukun Wang,¹ Danmei Zhang,¹ Jin Guo,¹ Qingqi Zhang,¹ Wenbin Zhang,³ and Zuojiong Gong^{1,5,*}

SUMMARY

The liver is the main organ associated with metabolism. In our previous studies, we identified that the metabolic enzymes malate dehydrogenase 1 (MDH1) and isocitrate dehydrogenase 1 (IDH1) were differentially expressed in ALF. The aim of this study was to explore the changes in the acetylation of MDH1 and IDH1 and the therapeutic effect of histone deacetylase (HDAC) inhibitor in acute liver failure (ALF). Decreased levels of many metabolites were observed in ALF patients. MDH1 and IDH1 were decreased in the livers of ALF patients. The HDAC inhibitor ACY1215 improved the expression of MDH1 and IDH1 after treatment with MDH1-siRNA and IDH1-siRNA. Transfection with mutant plasmids and adeno-associated viruses, identified MDH1 K118 acetylation and IDH1 K93 acetylation as two important sites that regulate metabolism *in vitro* and *in vivo*.

INTRODUCTION

Acute liver failure (ALF) is a critical disease characterized by severe synthesis, detoxification, and metabolism dysfunction. At present, there is still a lack of effective treatments for ALF.¹ The mechanism of ALF is complex. Inflammation, epigenetic regulation, intestinal flora, and mitochondrial energy metabolism may contribute to the pathogenesis and development of ALF. The liver is the main organ associated with metabolism. Hepatocytes are rich in mitochondria. As the main site of metabolism, the mitochondria of hepatocytes produce adenosine triphosphate (ATP), which provides energy for liver function.² Many pathogenic factors in the liver (viral infections, drugs, inflammation, and so on) can induce mitochondrial injury and dysfunction, mainly through tricarboxylic acid cycle disorders; thus, the rate of oxygen consumption in liver cells in the context of liver failure significantly decreased, and the expression of tricarboxylic acid cycle related genes is decreased.^{3,4} Abnormal liver function can be accompanied by serious energy metabolic disorders and malnutrition.⁵ Therefore, reducing mitochondrial damage in hepatocytes and restoring normal liver energy metabolism are important factors in the clinical treatment of liver failure.

In our previous studies, through quantitative protein sequencing experiments, we identified that the metabolic enzymes malate dehydrogenase 1 (MDH1) and isocitrate dehydrogenase 1 (IDH1) were differentially expressed in ALF.⁶ MDH1 and IDH1 are two important metabolic enzymes. MDH1 catalyzes the interconversion of malate and oxaloacetate in the cytoplasm using the coenzyme NAD/NADH, which plays an important role in cytosolic malate-aspartate shuttle.^{7,8} IDH1 catalyzes the interconversion of isocitrate and α -ketoglutarate in the cytoplasm using the coenzyme NADP/NADPH, which is widely involved in the metabolism of sugars, lipids, and amino acids in the liver.⁹ MDH1 and IDH1 perform electron transfer through redox reactions to maintain cytosolic NADH or NADPH balance. A decrease in the activity of MDH1 and IDH1 can cause abnormalities in the electron transfer, which can further affect metabolism and lead to energy metabolism disorders.^{10,11}

The roles of MDH1 and IDH1 have been reported in a variety of diseases. MDH1 is inactivated during acute lung injury. MDH1 can promote the viability of alveolar epithelial type II cells by promoting glucose intake, suggesting that targeting MDH1 may be a potential therapeutic strategy for patients with acute lung injury.¹² In addition, the MDH1-mediated malate-aspartate NADH shuttle maintains the activity levels of fetal liver hematopoietic stem cells.¹³ Recent studies have shown that MDH1 can regulate autophagy and is required to maintain the level of the autophagy promoter unc-51 like autophagy activating kinase 1 (ULK1), and the activity of MDH1 increases after autophagy induction. As a new autophagy regulator, MDH1 has been reported to be associated with pancreatic ductal adenocarcinoma.¹⁴ IDH1 has been shown to be downregulated in mice with chronic unpredictable stress. IDH1 gene knockout can inhibit cell proliferation, accelerate cell aging, increase reactive oxygen species (ROS) levels and induce autophagy through the mitogen-activated protein kinase (MAPK) signaling pathway. Therefore, increasing IDH1 activity may be an effective strategy for the treatment of ovarian dysfunction.¹⁵

Protein modifications (such as methylation and acetylation) of MDH1 and IDH1 can also affect diseases.^{16,17} Arginine methylation of MDH1 can inhibit glutamine metabolism and inhibit pancreatic cancer.¹⁸ Acetylation of MDH1 significantly enhances its activity, increases

¹Department of Infectious Diseases, Renmin Hospital of Wuhan University, Wuhan 430060, China

²Department of Cardiology, Wuhan No.1 Hospital, Wuhan Hospital of Traditional Chinese and Western Medicine, Wuhan 430022, China

³Department of Oncology, Renmin Hospital of Wuhan University, Wuhan 430060, China

⁴These authors contributed equally

⁵Lead contact

*Correspondence: zjgong@163.com

<https://doi.org/10.1016/j.isci.2024.109678>



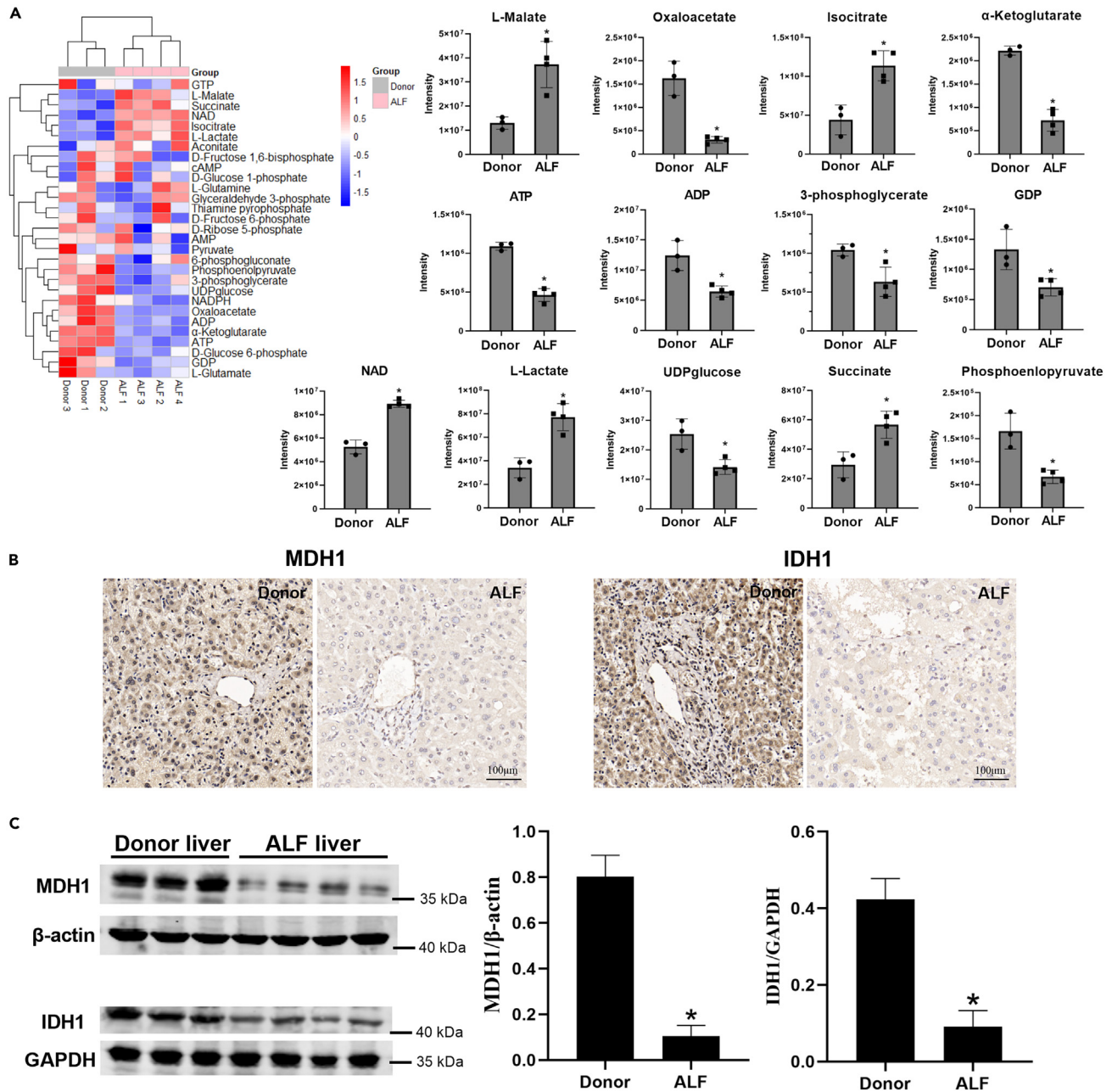


Figure 1. Energy metabolism in the liver tissue of ALF patients was disordered and the levels of MDH1 and IDH1 were decreased in the liver tissue of ALF patients

(A) Metabolites in three donor and four ALF human livers were examined by LC-MS/MS, and the levels of some metabolites are shown in bar charts.

(B) IHC analysis of MDH1 and IDH1 expression.

(C) Protein levels of MDH1 and IDH1 in human liver samples. The results are presented as mean \pm SD based on three repetitions. * Compared with the donor group, $p < 0.05$.

intracellular NADH levels, and promotes adipogenic differentiation, indicating that adipogenic differentiation may be regulated by MDH1 acetylation.¹⁶ IDH1 is highly acetylated in primary tumors and liver metastases of colorectal cancer. IDH1 acetylation can regulate intracellular metabolite concentrations, regulate cellular redox reactions, and control the progression of colorectal cancer.¹⁹ However, the role of MDH1 and IDH1 and their protein modifications in ALF remain unclear. Since MDH1 and IDH1 play important roles in regulating energy metabolism, it is particularly important to study the role and potential mechanism of MDH1, IDH1 and their protein modifications for the accurate diagnosis and treatment of ALF.

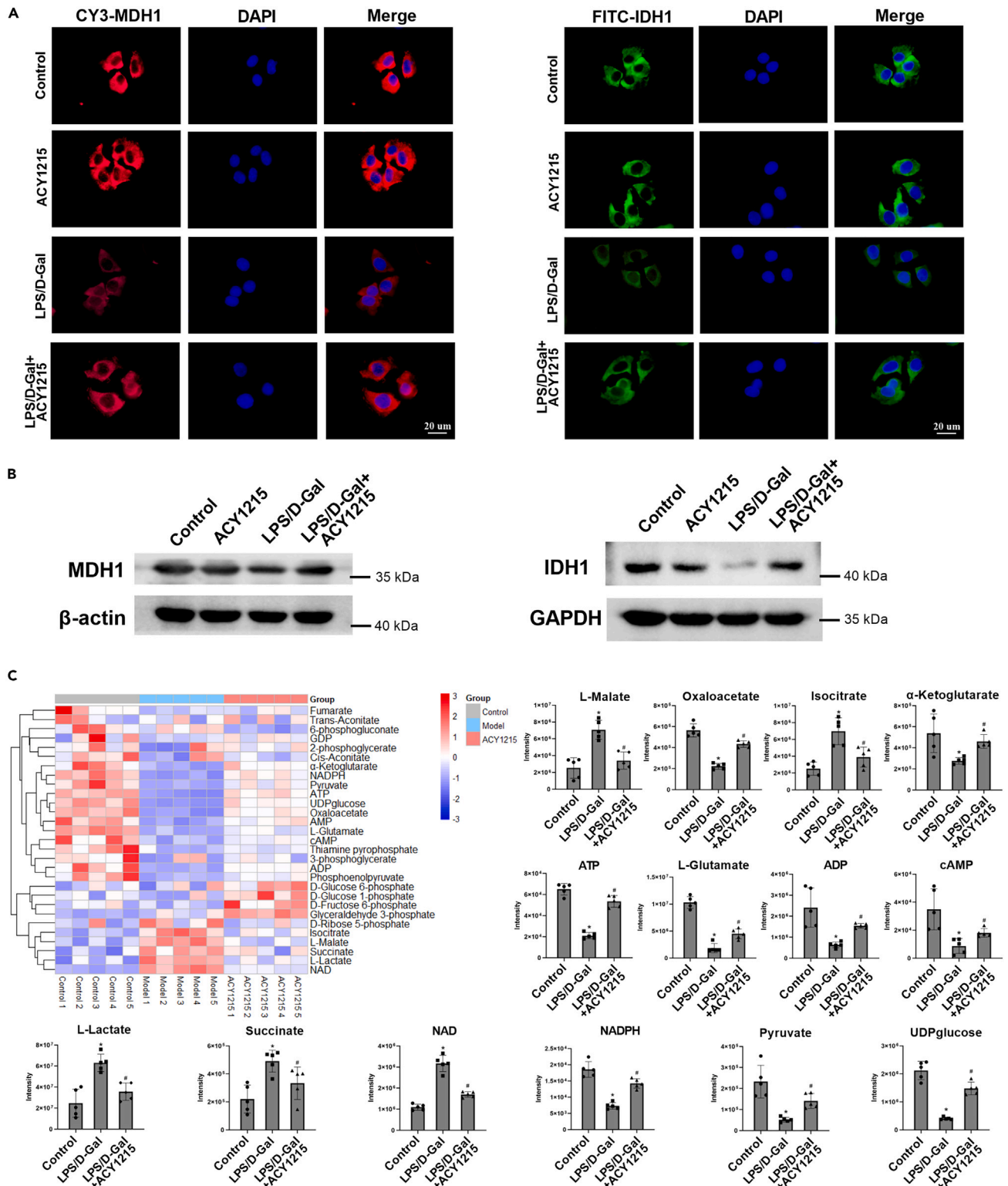


Figure 2. Continued

(A) IF analysis of MDH1 and IDH1 in AML-12 cells.

(B) Protein levels of MDH1 and IDH1 in each group.

(C) Metabolites were detected by LC-MS/MS, and the levels of some metabolites are shown in bar charts. The results are presented as the mean \pm SD. The LC-MS/MS results are based on five repetitions, and the other results are based on three repetitions. * Compared with the control group, $p < 0.05$; # compared with the LPS/D-Gal group, $p < 0.05$. In the heatmap, "Model" means "LPS/D-Gal group"; "ACY1215" means "LPS/D-Gal + ACY1215 group".

Histone acetylation is regulated by histone acetylase (HAT) and histone deacetylase (HDAC), which are in homeostasis. Histone acetylation means that HAT catalyses the transfer of negatively charged acetyl groups from acetyl-CoA to the amino terminus of lysine, thereby neutralizing the positive charge of histones and resulting in loose connections between DNA-histones and nucleosomes, which promotes the binding of transcription factors to DNA, and enables DNA transcription. HDAC can remove the acetyl group from histones, restore the positive charge, and promote the interaction between histones and negatively charged DNA, thereby leading to the condensation of chromatin structure, and inhibiting the transcription of DNA.

In this study, lipopolysaccharide (LPS)/D-galactosamine (D-Gal) was used to induce liver failure *in vitro* and *in vivo*. The roles of MDH1 and IDH1 and their acetylation were investigated by using various interventions, such as the HDAC inhibitor ACY1215, knocking down MDH1 and IDH1, constructing MDH1 and IDH1 lysine site mutant plasmids and adeno-associated viruses (AAVs). This study may provide a scientific basis for the accurate diagnosis and treatment of ALF.

RESULTS

Energy metabolism in the liver tissue of ALF patients was disordered and the levels of MDH1 and IDH1 were decreased in the liver tissue of ALF patients

The metabolomics of liver tissues from normal donors and ALF patients is shown in Figure 1A. We found that the total levels of many metabolites (ATP, adenosine diphosphate (ADP), phosphoenolpyruvate, guanosine diphosphate (GDP), UDPglucose, 3-phosphoglycerate, oxaloacetate, and α -ketoglutarate etc.) were decreased, indicating that energy metabolism in the liver tissue of ALF patients was inhibited compared with that in donor livers. There are many enzymes that can affect the levels of these metabolites. Based on our previous studies, the protein quantitative sequencing results showed that only MDH1 and IDH1 were differently expressed among normal, LPS/D-Gal and ACY1215 groups.⁶ Therefore, we focused on MDH1 and IDH1 in subsequent experiments. The levels of MDH1 and IDH1 in the liver tissue of ALF patients were examined. The levels of MDH1 and IDH1 were decreased as shown in Figures 1B and 1C.

The HDAC inhibitor ACY1215 increased the expression of MDH1 and IDH1 and improved energy metabolism in AML-12 cells

MDH1 and IDH1 have been reported to be modified by acetylation, thus, the HDAC inhibitor ACY1215 was used in this study. The results showed that ACY1215 increased the expression of MDH1 and IDH1 (Figures 2A and 2B) in AML-12 cells compared with those in the LPS/D-Gal group. The total levels of metabolites were also detected. The results showed that ACY1215 increased the total levels of many metabolites (oxaloacetate, α -ketoglutarate, ATP, ADP, phosphoenolpyruvate, GDP, UDPglucose, 3-phosphoglycerate, etc.) compared with those in the LPS/D-Gal group (Figure 2C). These results indicated that the HDAC inhibitor ACY1215 could improve metabolism by affecting MDH1 and IDH1.

ACY1215 rescued MDH1 and IDH1 expression after treatment with MDH1-siRNA and IDH1-siRNA in AML-12 cells

MDH1-siRNA and IDH1-siRNA significantly decreased the expression of MDH1 and IDH1. ACY1215 rescued MDH1 and IDH1 expression after treatment with MDH1-siRNA and IDH1-siRNA in AML-12 cells (Figure 3A). In addition, the total levels of metabolites (oxaloacetate, α -ketoglutarate, ATP, ADP, phosphoenolpyruvate, GDP, UDPglucose, cAMP, etc.) in LPS/D-Gal + MDH1-siRNA/IDH1-siRNA group were significantly decreased compared with those in the LPS/D-Gal group. ACY1215 increased these metabolites levels compared with those in the LPS/D-Gal + MDH1-siRNA/IDH1-siRNA group (Figures 3B and 3C). These results further indicated that the HDAC inhibitor ACY1215 could improve metabolism by affecting MDH1 and IDH1.

Acetylation of the MDH1 K118 and IDH1 K93 sites is associated with the activities of MDH1 and IDH1 in AML-12 cells

The acetylation levels of MDH1 and IDH1 in ALF were examined. The IP results showed that MDH1 and IDH1 had acetylated lysine residues (Figure 4A). By consulting the literature and the UniProt database,^{16,17,19-22} we screened the sites K107, K118, K239, and K298 of MDH1 and K81, K93, K224, K233, and K321 of IDH1 in this study. A lack of acetylation was simulated by mutating lysine (K) to arginine (R), which is a widely used method in previous studies.^{23,24} We first transfected the mutant plasmids into 293T cells for extensive screening. The results showed that the acetylation levels of MDH1 and IDH1 were significantly decreased by MDH1 K118 and IDH1 K93 and K224 mutations, respectively (Figure 4B). We further verified this outcome in AML-12 cells stimulated by LPS/D-Gal and used ACY1215 as a treatment. The results showed that MDH1 K118 mutation and IDH1 K93 mutation significantly decreased the acetylation and activities of MDH1 and IDH1. MDH1 K118 mutation (LPS/D-Gal + ACY1215 + MDH1 K118R group) decreased the acetylation of MDH1 compared with

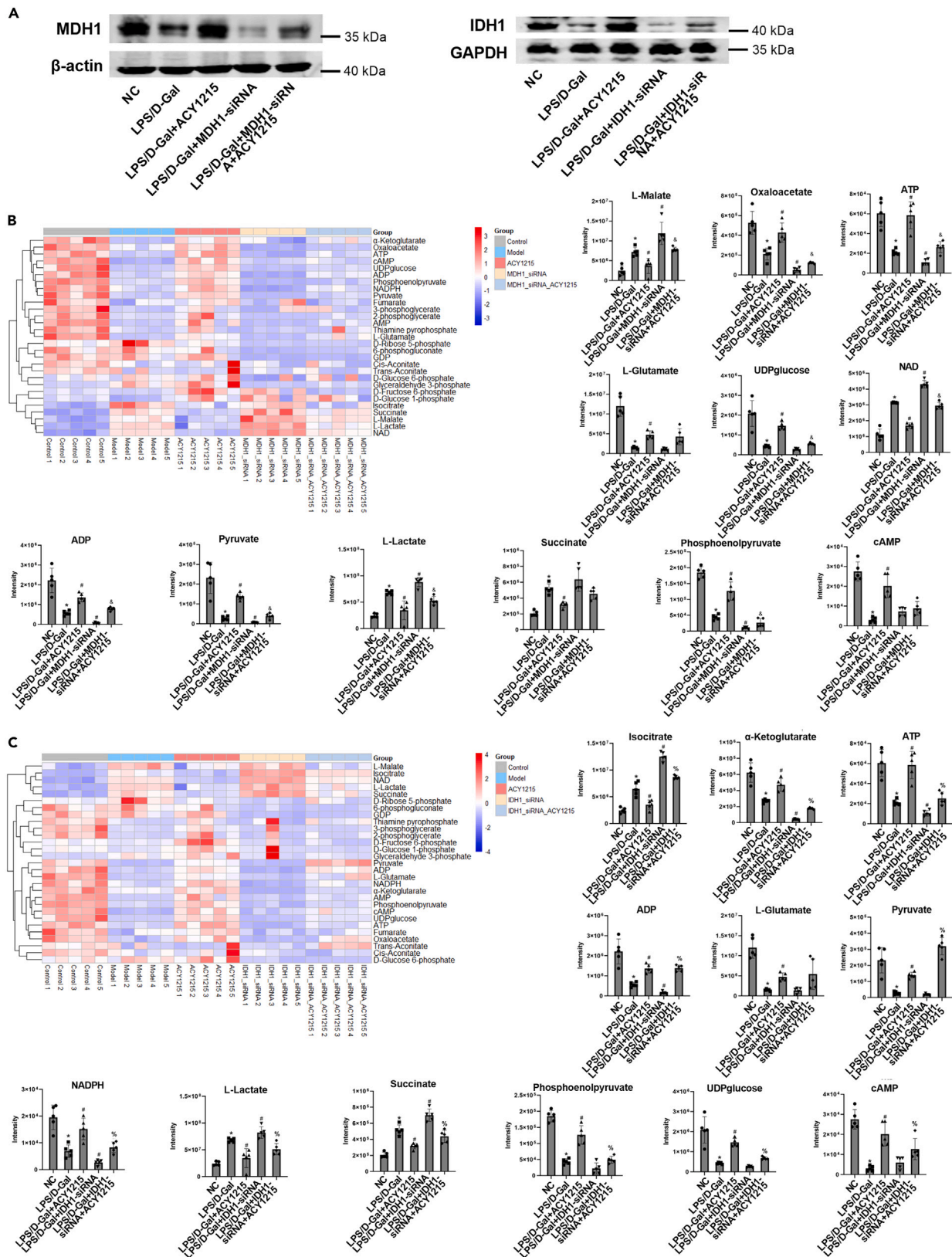


Figure 3. After the application of MDH1-siRNA and IDH1-siRNA, the improvement effect of ACY1215 on metabolism was weakened in AML-12 cells

The cells were divided into the NC group, LPS/D-Gal group, LPS/D-Gal + ACY1215 group, LPS/D-Gal + MDH1-siRNA or IDH1-siRNA group, and LPS/D-Gal + ACY1215 + MDH1-siRNA or LPS/D-Gal + ACY1215 + IDH1-siRNA group. LPS/D-Gal was used to stimulate the cells except the NC group. MDH1-siRNA or IDH1-siRNA transfection was performed 24 h prior to LPS/D-Gal stimulation, and ACY1215 was added to the medium 2 h prior to LPS/D-Gal stimulation. The cells were harvested 24 h after LPS/D-Gal administration.

(A) Protein levels of MDH1 and IDH1 in each group.

(B and C) Metabolites were detected by LC-MS/MS, and the levels of some metabolites are shown in bar charts. The results are presented as the mean \pm SD. The LC-MS/MS results are based on five repetitions, and the other results are based on three repetitions. * Compared with NC group, $p < 0.05$; # compared with LPS/D-Gal group, $p < 0.05$; & compared with LPS/D-Gal + MDH1-siRNA group, $p < 0.05$; % compared with LPS/D-Gal + IDH1-siRNA group, $p < 0.05$. In the heatmap, "Control" means "NC group"; "Model" means "LPS/D-Gal group"; "ACY1215" means "LPS/D-Gal + ACY1215 group"; "MDH1_siRNA" means "LPS/D-Gal + MDH1-siRNA group"; "IDH1_siRNA" means "LPS/D-Gal + IDH1-siRNA group"; "MDH1_siRNA_ACY1215" means "LPS/D-Gal + ACY1215 + MDH1-siRNA group"; and "IDH1_siRNA_ACY1215" means "LPS/D-Gal + ACY1215 + IDH1-siRNA group".

that in the LPS/D-Gal + ACY1215 group. Similar results were observed in response to the IDH1 K93 mutation. However, the acetylation of IDH1 was not significantly weakened by the IDH1 K224 mutation compared with that in the LPS/D-Gal + ACY1215 group. These results indicated that ACY1215 may regulate the acetylation and activities of MDH1 and IDH1 by acting on the MDH1 K118 and IDH1 K93 sites (Figures 4C–E). The protein structures of MDH1 K118 and IDH1 K93 are shown in Figure 4F.

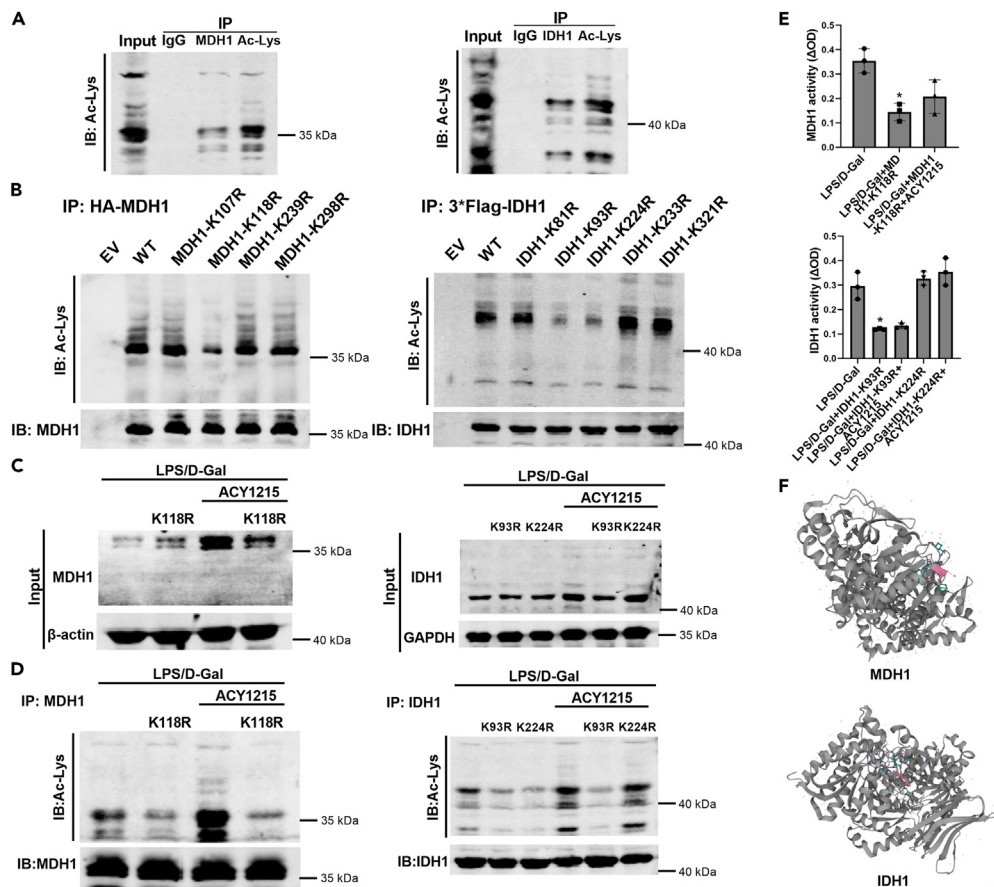


Figure 4. Acetylation of the MDH1 K118 site and IDH1 K93 site plays key roles in activity in cells

293T cells were seeded into 6-well plates and transfected with plasmids mixed with Lipofectamine 2000 according to the manufacturer's instructions. For AML-12 cells, LPS/D-Gal and ACY1215 were used to stimulate the cells after plasmid transfection as described above.

(A) IP analysis of MDH1 and IDH1 acetylation in AML-12 cells.

(B) IP analysis of 293T cells after plasmid transfection.

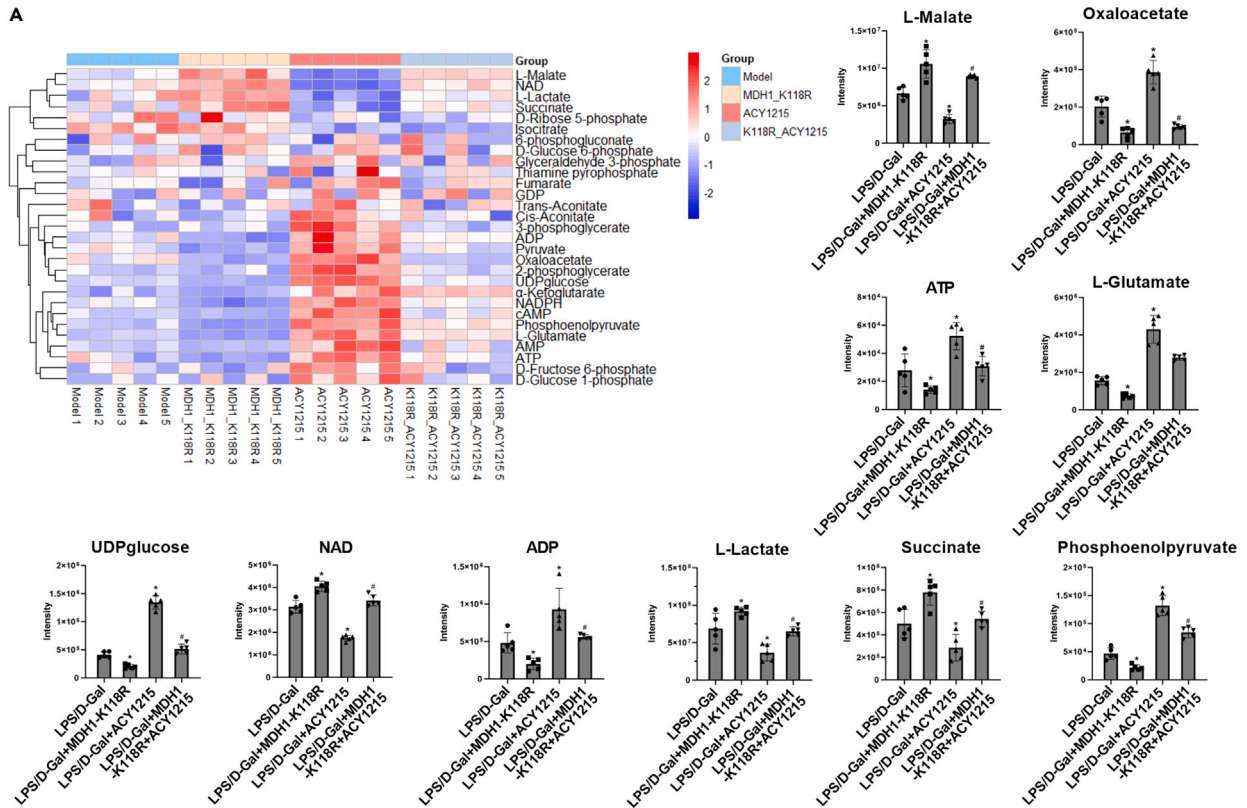
(C) Protein levels of MDH1 and IDH1 in AML-12 cells.

(D) IP analysis of AML-12 cells after plasmid transfection and drug treatment.

(E) The activities of MDH1 and IDH1 in each group. MDH1 or IDH1 levels were normalized.

(F) Structure of MDH1 K118 (UniProt database: P40925) and IDH1 K93 (UniProt database: O75874). * Compared with LPS/D-Gal group, $p < 0.05$.

A



B

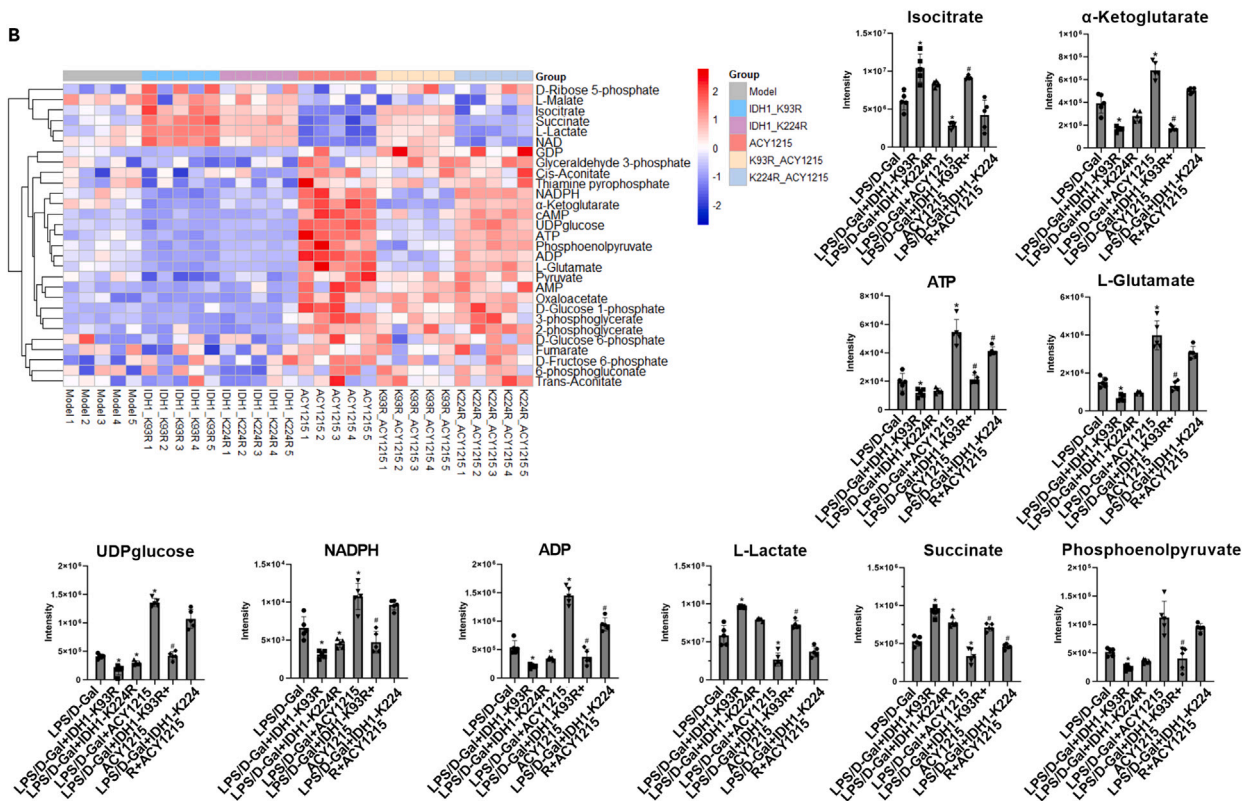


Figure 5. Effect of MDH1 K118 acetylation and IDH1 K93 and K224 acetylation on energy metabolism in AML-12 cells

(A and B) Metabolites were detected by LC-MS/MS, and the levels of some metabolites are shown in bar charts. The results are presented as the mean \pm SD based on five repetitions. * Compared with the LPS/D-Gal group, $p < 0.05$; # compared with the LPS/D-Gal + ACY1215 group, $p < 0.05$. In the heatmap, "Model" means "LPS/D-Gal group"; "ACY1215" means "LPS/D-Gal + ACY1215 group"; "MDH1_K118R" means "LPS/D-Gal + MDH1 K118R group"; "K118R_ACY1215" means "LPS/D-Gal + MDH1 K118R + ACY1215 group"; "IDH1_K93R" means "LPS/D-Gal + IDH1 K93R group"; "IDH1_K224R" means "LPS/D-Gal + IDH1 K224R group"; "K93R_ACY1215" means "LPS/D-Gal + IDH1 K93R + ACY1215 group"; and "K224R_ACY1215" means "LPS/D-Gal + IDH1 K224R + ACY1215 group".

Effects of acetylation of MDH1 K118 and IDH1 K93 and K224 on energy metabolism in AML-12 cells

The effects of acetylation of MDH1 K118 and IDH1 K93 and K224 on energy metabolism in AML-12 cells were examined by transfecting MDH1 K118R and IDH1 K93R and K224R mutant plasmids. The results showed that the MDH1 K118 mutation decreased the total levels of ATP, oxaloacetate, L-glutamate, UDPglucose, ADP, phosphoenolpyruvate, and other metabolites, indicating that energy metabolism was inhibited (Figure 5A). Similar results were observed in response to the IDH1 K93 mutation. The IDH1 K224 mutation also inhibited energy metabolism to a slight extent (Figure 5B).

MDH1 K118 and IDH1 K93 mutations aggravated liver damage in mice

The mice were injected with MDH1-K118R and IDH1-K93R AAVs to study the effects of the acetylation of MDH1 K118 and IDH1 K93 *in vivo*. The mutation site was verified first. As shown in Figure 6A, strong AAV fluorescence was observed in frozen sections of mouse liver tissues, and the levels of acetylation were decreased in response to the MDH1 K118 and IDH1 K93 mutations (Figure 6B). These results indicated successful mutation. In addition, after the mutation of MDH1 K118 and IDH1 K93, the acetylation of MDH1 and IDH1 was decreased compared with those in the LPS/D-Gal + ACY1215 group (Figure 6C). Histological HE examination and liver function analysis showed that MDH1-K118R and IDH1-K93R aggravated liver damage and weakened the protective effect of ACY1215 on the liver (Figures 6D and 6E).

Effects of acetylation of MDH1 K118 and IDH1 K93 on energy metabolism in mouse livers

The effects of MDH1 K118 and IDH1 K93 acetylation on energy metabolism in mouse livers were also detected. The results showed that MDH1-K118R decreased the total levels of metabolites such as ATP, oxaloacetate, L-glutamate, UDPglucose, ADP, and phosphoenolpyruvate, indicating the inhibition of energy metabolism. Moreover, the protective effect of ACY1215 on liver energy metabolism was attenuated by MDH1-K118R (Figure 7A). Similar results were also observed in response to the IDH1 K93 mutation (Figure 7B). Thus, these results indicated that MDH1 K118 and IDH1 K93 acetylation are involved in liver energy metabolism.

DISCUSSION

It has been reported that a total of 1047 proteins can be modified by acetylation, and these proteins have been identified in the liver. Most of them are non-histones and energy metabolic enzymes. They can be modified by acetylation in nonhistone forms.¹⁷ MDH1 and IDH1 are two key enzymes that can also be modified by acetylation. In this study, energy metabolism was inhibited in the liver tissue of patients with ALF. The levels of MDH1 or IDH1 were decreased in ALF patients. These results suggest that MDH1 and IDH1 are associated with ALF. Recent studies have reported that MDH1 and IDH1 were markedly changed in some diseases. The function of MDH1 in the brains of old mice was significantly reduced.²⁵ Knockout of MDH1 downregulated the expression of genes related to osteoclast differentiation and reduced the formation of osteoclasts. After MDH1 knockout, the production of intracellular ATP was reduced, suggesting that MDH1 plays a key role in osteoclast differentiation by regulating intracellular energy status.²⁶ IDH1 is crucial for metabolism in the liver. Compared with those of wild-type mice, blood glucose levels of IDH1-deficient mice were decreased, and blood glycine and alanine levels were increased. IDH1-deficient cells had increased glucose consumption, decreased intracellular glutamate and α -ketoglutarate acid levels, and decreased alanine utilization. The expression levels of genes involved in metabolism were decreased in IDH1-deficient livers. Therefore, IDH1 is essential for metabolism *in vivo*.²⁷

Our results also showed that the HDAC inhibitor ACY1215 could increase the acetylation and activities of MDH1 and IDH1 and improve liver metabolism, suggesting that the acetylation of MDH1 and IDH1 might be related to the occurrence and development of ALF. Two possible mechanisms may explain how HDAC inhibitors affect MDH1 and IDH1. On the one hand, HDAC inhibitors lead to loose connections between DNA histones and nucleosomes, which promotes protein expression. On the other hand, the higher levels of MDH1 and IDH1 induced by ACY1215 may result from higher stability and less degradation when the proteins are more acetylated. A previous study reported the role of MDH1 and IDH1 acetylation in adipogenic differentiation and mammalian cancer, respectively.^{16,19} HDAC6 can bind to MDH1 and mediate the deacetylation of MDH1. MDH1 acetylation is inhibited when cells are stimulated by damage, but is increased when HDAC6 is inhibited, suggesting an interaction between HDAC6 and MDH1.²⁸ In our study, the acetylation of MDH1 was directly affected by the HDAC6 inhibitor ACY 1215.

In the physiological state, the acetylation and deacetylation of MDH1 or IDH1 are in balance. In the pathological state, this balance is broken, and the function of MDH1 or IDH1 can be affected, which may lead to metabolic disorders. In this study, we further constructed mutant plasmids and adeno-associated viruses to investigate the role of MDH1 and IDH1 acetylation in ALF. The results showed that MDH1 K118R and IDH1 K93R significantly reduced the acetylation and activities of MDH1 and IDH1, indicating that the acetylation of MDH1 K118 and IDH1 K93 was important for their activities and function. Studies have reported that the acetylation of K121, K298 and K118 sites relates to the activity of MDH1 in adipogenic differentiation and the acetylation of K224 relates to the activity of IDH1 in colorectal

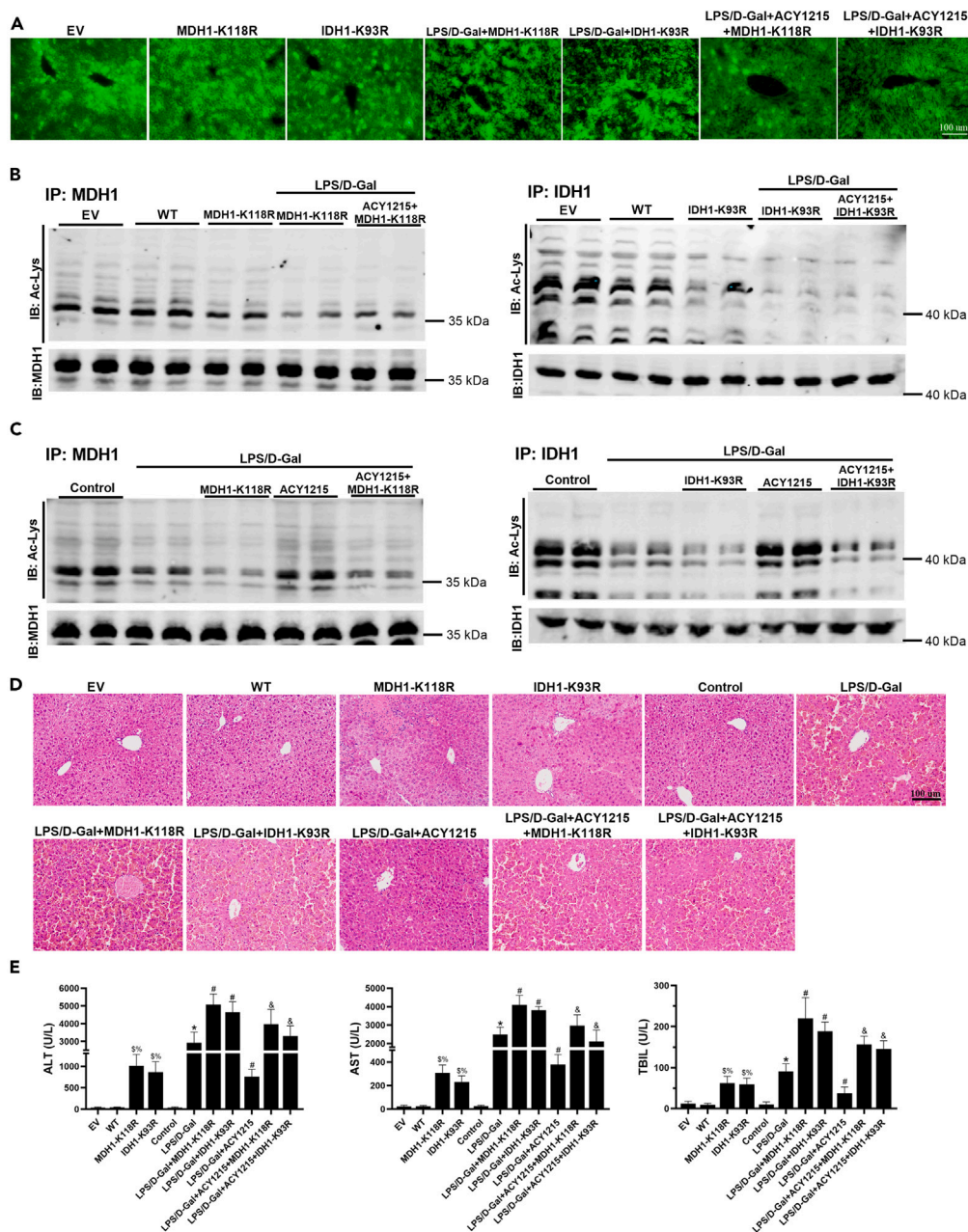


Figure 6. The MDH1 K118 mutation and IDH1 K93 mutation aggravated liver damage in mice

The mice were randomly divided into eleven groups: empty (EV) group, wild-type (WT) group, MDH1-K118R group, IDH1-K93R group, control group, LPS/D-Gal group, LPS/D-Gal + MDH1-K118R group, LPS/D-Gal + IDH1-K93R group, LPS/D-Gal + ACY1215 group, LPS/D-Gal + ACY1215 + MDH1-K118R group, and LPS/D-Gal + ACY1215 + IDH1-K93R group. Except for the EV, WT, MDH1-K118R, IDH1-K93R and control groups, the mice were intraperitoneally injected with LPS (100 μ g/kg) and D-Gal (400 mg/kg). AAV was administered via tail vein injection at a dose of 1×10^{11} vg 4 weeks before LPS/D-Gal injection. ACY1215 (25 mg/kg) was administered by intraperitoneal injection 2 h before LPS/D-Gal injection. At 24 h after LPS/D-Gal injection, the mice were sacrificed. Mouse livers and serum were collected for analysis.

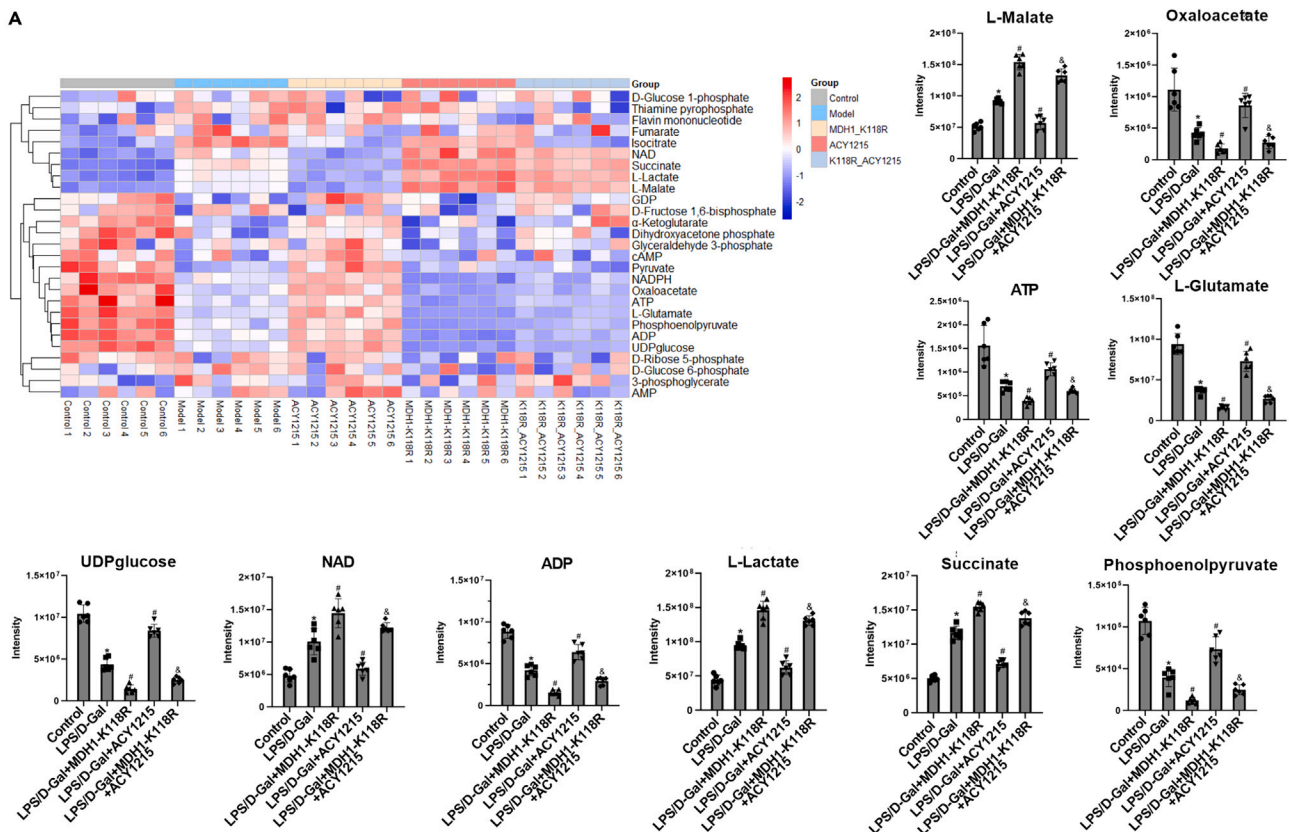
(A) Representative images showing AAV fluorescence.

(B and C) IP analysis of MDH1 and IDH1 acetylation in each group.

(D) HE staining in each group.

(E) The levels of serum ALT, AST, and TBIL in each group. The results are presented as the mean \pm SD based on three repetitions. \$ Compared with the EV group, $p < 0.05$; % compared with the WT group, $p < 0.05$; * compared with the control group, $p < 0.05$; # compared with the LPS/D-Gal group, $p < 0.05$; & compared with the LPS/D-Gal + ACY1215 group, $p < 0.05$.

A



B

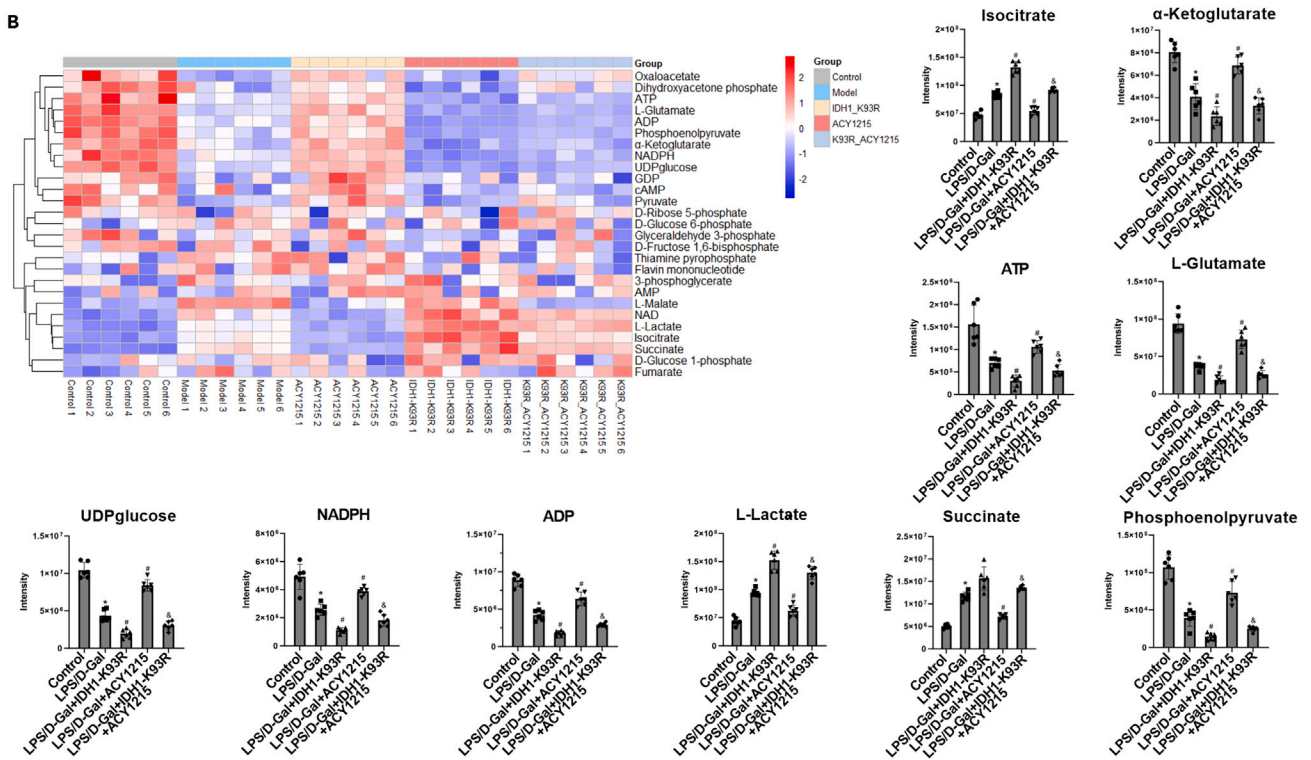


Figure 7. Effect of MDH1 K118 acetylation and IDH1 K93 acetylation on energy metabolism in mouse livers

(A and B) Metabolites were detected by LC-MS/MS, and the levels of some metabolites are presented as the mean \pm SD. * Compared with the control group, $p < 0.05$; # compared with the LPS/D-Gal group, $p < 0.05$; & compared with the LPS/D-Gal + ACY1215 group, $p < 0.05$. In the heatmap, "Model" means "LPS/D-Gal group"; "ACY1215" means "LPS/D-Gal + ACY1215 group"; "MDH1_K118R" means "LPS/D-Gal + MDH1 K118R group"; "K118R_ACY1215" means "LPS/D-Gal + MDH1 K118R + ACY1215 group"; "IDH1_K93R" means "LPS/D-Gal + IDH1 K93R group"; and "K93R_ACY1215" means "LPS/D-Gal + IDH1 K93R + ACY1215 group".

cancer.^{16,19} This suggests that post-translational modification of proteins has a complex and special regulatory pattern. Research performed by Venkat et al. confirmed this.²¹ The researchers introduced acetylation modifications at eight sites, and the results showed that acetylation at different sites had different effects on IDH activity. Acetylation at K55, K142, K177, K242 and K350 increased IDH activity, while acetylation at K100, K230 and K235 decreased IDH activity.²¹ Besides, under different stimulus and intervention conditions, posttranslational modification may have different effects. For example, the stability of ULK1 can be regulated by ubiquitylation or deubiquitylation under the action of different enzymes.^{29,30} Therefore, acetylation may have different effects under different conditions.

Our results also showed that MDH1 K118R and IDH1 K93R inhibited energy metabolism, resulting in reductions in a variety of metabolites, such as ATP, L-glutamate, UDPglucose, ADP and phosphoenolpyruvate. Although MDH1 and IDH1 are mainly located in the cytoplasm and are not the main enzymes in the tricarboxylic acid (TCA) cycle, studies have reported that MDH1 is important in transporting NADH equivalents across the mitochondrial membrane, controlling TCA cycle pool size and affect the levels of a variety of metabolites,^{10,31} the production of ATP²⁶ and glucose depletion.³² Besides, IDH1-mutant cells exhibited increased oxidative tricarboxylic acid metabolism.¹¹ These results indicated that MDH1 and IDH1 are closely associated with energy metabolism. When energy production is insufficient to maintain the normal physiological function of the liver, liver dysfunction occurs. In addition, when the TCA cycle is disrupted, glucose enters the glycolytic pathway to produce pyruvate and ATP, which can be converted to acetyl-CoA and oxaloacetate. Acetyl-CoA and oxaloacetate can be used to synthesize citrate in mitochondria. When the concentration of citrate in mitochondria is high, citrate can be transported to the cytoplasm. Cytosolic citrate can be further decomposed into acetyl-CoA and oxaloacetate.¹⁶ Although this process can be compensated by the glycolytic pathway to produce oxaloacetate, the glycolytic pathway is in a state of failure when ALF occurs. Therefore, when ALF occurs, large numbers of mitochondria are destroyed, the TCA cycle and energy metabolism are impaired, MDH1 and IDH1 activities are decreased, and acetylation levels are reduced, which further aggravates metabolic disorders and damages liver function. Further liver damage can aggravate inflammation and promote the progression of disease. Therefore, energy metabolism and acetylation affect each other during ALF, and in-depth study of the mechanism is expected to provide new ideas for the diagnosis and treatment of ALF.

In conclusion, the acetylation of MDH1 and IDH1 is involved in the dysfunction of liver energy metabolism. Acetylation of MDH1 K118 and IDH1 K93 is associated with energy metabolism in ALF. HDAC inhibitor ACY1215 is expected to be an effective drug for the treatment of ALF.

Limitations of the study

There are some limitations to our study currently. We performed some experiments on cells and animals, but the number of clinical samples is small and prospective studies are lacking. Future studies will involve collecting more clinical samples for more detailed analysis of MDH1 and IDH1 acetylation. We will pay attention to expanding clinical samples and increasing *in vivo* and *in vitro* validation experiments, as well as refining the acquisition of clinical tissues, paying attention to the reproducibility of validation and the timeliness and accuracy of data acquisition in the future.

STAR★METHODS

Detailed methods are provided in the online version of this paper and include the following:

- KEY RESOURCES TABLE
- RESOURCE AVAILABILITY
 - Lead contact
 - Materials availability
 - Data and code availability
- EXPERIMENTAL MODEL AND SUBJECT DETAILS
 - Cell culture and treatment
 - Animal groups
 - Clinical specimen collection
- METHOD DETAILS
 - siRNA transfection
 - Plasmid transfection
 - Detection of energy metabolites
 - Immunofluorescence (IF)
 - Western blotting and immunoprecipitation (IP)
 - Detection of the activities of MDH1 and IDH1

- Hematoxylin-eosin (HE) staining and immunohistochemistry (IHC)
- Detection of ALT, AST and TBIL
- QUANTIFICATION AND STATISTICAL ANALYSIS

SUPPLEMENTAL INFORMATION

Supplemental information can be found online at <https://doi.org/10.1016/j.isci.2024.109678>.

ACKNOWLEDGMENTS

This work was supported by the National Natural Science Foundation of China (82070609 and 82270627).

AUTHOR CONTRIBUTIONS

C.S.: methodology, data curation, writing—original draft preparation; Y.Z.: methodology, data curation, writing—original draft preparation; Q.C.: formal analysis, writing—review and editing; Y.W.: formal analysis, writing—review and editing; D.Z.: investigation, validation; J.G.: investigation, validation; Q.Z.: investigation, validation; W.Z.: investigation, validation; Z.G.: conceptualization, supervision, funding acquisition. All authors read and approved the final manuscript.

DECLARATION OF INTERESTS

The authors declare that they have no competing of interests.

Received: January 18, 2024

Revised: February 19, 2024

Accepted: April 3, 2024

Published: April 6, 2024

REFERENCES

1. Stravitz, R.T., and Lee, W.M. (2019). Acute liver failure. *Lancet* 394, 869–881. [https://doi.org/10.1016/S0140-6736\(19\)31894-X](https://doi.org/10.1016/S0140-6736(19)31894-X).
2. Wu, M., Liao, L., Jiang, L., Zhang, C., Gao, H., Qiao, L., Liu, S., and Shi, D. (2019). Liver-targeted Nano-MitoPBN normalizes glucose metabolism by improving mitochondrial redox balance. *Biomaterials* 222, 119457. <https://doi.org/10.1016/j.biomaterials.2019.119457>.
3. Nishikawa, T., Bellance, N., Damm, A., Bing, H., Zhu, Z., Handa, K., Yovchev, M.I., Sehgal, V., Moss, T.J., Oertel, M., et al. (2014). A switch in the source of ATP production and a loss in capacity to perform glycolysis are hallmarks of hepatocyte failure in advance liver disease. *J. Hepatol.* 60, 1203–1211. <https://doi.org/10.1016/j.jhep.2014.02.014>.
4. Mansouri, A., Gattolliat, C.H., and Asselah, T. (2018). Mitochondrial Dysfunction and Signaling in Chronic Liver Diseases. *Gastroenterology* 155, 629–647. <https://doi.org/10.1053/j.gastro.2018.06.083>.
5. Meng, Q.H., Hou, W., Yu, H.W., Lu, J., Li, J., Wang, J.H., Zhang, F.Y., Zhang, J., Yao, Q.W., Wu, J., et al. (2011). Resting energy expenditure and substrate metabolism in patients with acute-on-chronic hepatitis B liver failure. *J. Clin. Gastroenterol.* 45, 456–461. <https://doi.org/10.1097/MCG.0b013e31820f7f02>.
6. Wang, Y., Li, X., Chen, Q., Jiao, F., Shi, C., Pei, M., Wang, L., and Gong, Z. (2021b). Histone Deacetylase 6 Regulates the Activation of M1 Macrophages by the Glycolytic Pathway During Acute Liver Failure. *J. Inflamm. Res.* 14, 1473–1485. <https://doi.org/10.2147/JIR.S302391>.
7. Minárik, P., Tomásková, N., Kollárová, M., and Antalík, M. (2002). Malate dehydrogenases—structure and function. *Gen. Physiol. Biophys.* 21, 257–265. <https://pubmed.ncbi.nlm.nih.gov/12537350/>.
8. Broeks, M.H., van Karnebeek, C.D.M., Wanders, R.J.A., Jans, J.J.M., and Verhoeven-Duif, N.M. (2021). Inborn disorders of the malate aspartate shuttle. *J. Inher. Metab. Dis.* 44, 792–808. <https://doi.org/10.1002/jimd.12402>.
9. Yang, H.C., Yu, H., Liu, Y.C., Chen, T.L., Stern, A., Lo, S.J., and Chiu, D.T.Y. (2019). IDH-1 deficiency induces growth defects and metabolic alterations in GSPD-1-deficient *Caenorhabditis elegans*. *J. Mol. Med.* 97, 385–396. <https://doi.org/10.1007/s00109-018-01740-2>.
10. Lo, A.S.Y., Liew, C.T., Ngai, S.M., Tsui, S.K.W., Fung, K.P., Lee, C.Y., and Wayne, M.M.Y. (2005). Developmental regulation and cellular distribution of human cytosolic malate dehydrogenase (MDH1). *J. Cell. Biochem.* 94, 763–773. <https://doi.org/10.1002/jcb.20343>.
11. Grassian, A.R., Parker, S.J., Davidson, S.M., Divakaruni, A.S., Green, C.R., Zhang, X., Slocum, K.L., Pu, M., Lin, F., Vickers, C., et al. (2014). IDH1 mutations alter citric acid cycle metabolism and increase dependence on oxidative mitochondrial metabolism. *Cancer Res.* 74, 3317–3331. <https://doi.org/10.1158/0008-5472.CAN-14-0772-T>.
12. Hu, M., Yang, J., Xu, Y., and Liu, J. (2022). MDH1 and MDH2 Promote Cell Viability of Primary AT2 Cells by Increasing Glucose Uptake. *Comput. Math. Methods Med.* 2022, 2023500. <https://doi.org/10.1155/2022/2023500>.
13. Gu, H., Chen, C., Hao, X., Su, N., Huang, D., Zou, Y., Lin, S.H., Chen, X., Zheng, D., Liu, L., et al. (2020). MDH1-mediated malate-aspartate NADH shuttle maintains the activity levels of fetal liver hematopoietic stem cells. *Blood* 136, 553–571. <https://doi.org/10.1182/blood.2019003940>.
14. New, M., Van Acker, T., Sakamaki, J.I., Jiang, M., Saunders, R.E., Long, J., Wang, V.M.Y., Behrens, A., Cerveira, J., Sudhakar, P., et al. (2019). MDH1 and MPP7 Regulate Autophagy in Pancreatic Ductal Adenocarcinoma. *Cancer Res.* 79, 1884–1898. <https://doi.org/10.1158/0008-5472.CAN-18-2553>.
15. Sun, J., Guo, Y., Fan, Y., Wang, Q., Zhang, Q., and Lai, D. (2021). Decreased expression of IDH1 by chronic unpredictable stress suppresses proliferation and accelerates senescence of granulosa cells through ROS activated MAPK signaling pathways. *Free Radic. Biol. Med.* 169, 122–136. <https://doi.org/10.1016/j.freeradbiomed.2021.04.016>.
16. Kim, E.Y., Kim, W.K., Kang, H.J., Kim, J.H., Chung, S.J., Seo, Y.S., Park, S.G., Lee, S.C., and Bae, K.H. (2012). Acetylation of malate dehydrogenase 1 promotes adipogenic differentiation via activating its enzymatic activity. *J. Lipid Res.* 53, 1864–1876. <https://doi.org/10.1194/jlr.M026567>.
17. Zhao, S., Xu, W., Jiang, W., Yu, W., Lin, Y., Zhang, T., Yao, J., Zhou, L., Zeng, Y., Li, H., et al. (2010). Regulation of cellular metabolism by protein lysine acetylation. *Science* 327, 1000–1004. <https://doi.org/10.1126/science.1179689>.
18. Wang, Y.P., Zhou, W., Wang, J., Huang, X., Zuo, Y., Wang, T.S., Gao, X., Xu, Y.Y., Zou, S.W., Liu, Y.B., et al. (2016). Arginine Methylation of MDH1 by CARM1 Inhibits Glutamine Metabolism and Suppresses Pancreatic Cancer. *Mol. Cell* 64, 673–687. <https://doi.org/10.1016/j.molcel.2016.09.028>.
19. Wang, B., Ye, Y., Yang, X., Liu, B., Wang, Z., Chen, S., Jiang, K., Zhang, W., Jiang, H., Mustonen, H., et al. (2020). SIRT2-dependent

- IDH1 deacetylation inhibits colorectal cancer and liver metastases. *EMBO Rep.* 21, e48183. <https://doi.org/10.15252/embr.201948183>.
20. Shen, Z., Wang, B., Luo, J., Jiang, K., Zhang, H., Mustonen, H., Puolakkainen, P., Zhu, J., Ye, Y., and Wang, S. (2016). Global-scale profiling of differential expressed lysine acetylated proteins in colorectal cancer tumors and paired liver metastases. *J. Proteomics* 142, 24–32. <https://doi.org/10.1016/j.jprot.2016.05.002>.
 21. Venkat, S., Chen, H., Stahman, A., Hudson, D., McGuire, P., Gan, Q., and Fan, C. (2018). Characterizing Lysine Acetylation of Isocitrate Dehydrogenase in *Escherichia coli*. *J. Mol. Biol.* 430, 1901–1911. <https://doi.org/10.1016/j.jmb.2018.04.031>.
 22. Wang, Q., Zhang, Y., Yang, C., Xiong, H., Lin, Y., Yao, J., Li, H., Xie, L., Zhao, W., Yao, Y., et al. (2010). Acetylation of metabolic enzymes coordinates carbon source utilization and metabolic flux. *Science* 327, 1004–1007. <https://doi.org/10.1126/science.1179687>.
 23. Khattar, V., and Thottassery, J.V. (2015). Cks1 proteasomal turnover is a predominant mode of regulation in breast cancer cells: role of key tyrosines and lysines. *Int. J. Oncol.* 46, 395–406. <https://doi.org/10.3892/ijo.2014.2728>.
 24. Obeng, E., Lei, J., Ngowo, J., Mao, F., Yan, H., Zhu, Y., and Yu, W. (2021). Acetylation of nucleopolyhedrovirus P35 is crucial for its anti-apoptotic activity in silkworm, *Bombyx mori*. *Acta Virol.* 65, 264–272. https://doi.org/10.4149/av_2021_303.
 25. Guo, X., Park, J.E., Gallart-Palau, X., and Sze, S.K. (2020). Oxidative Damage to the TCA Cycle Enzyme MDH1 Dysregulates Bioenergetic Enzymatic Activity in the Aged Murine Brain. *J. Proteome Res.* 19, 1706–1717. <https://doi.org/10.1021/acs.jproteome.9b00861>.
 26. Oh, S.J., Gu, D.R., Jin, S.H., Park, K.H., and Lee, S.H. (2016). Cytosolic malate dehydrogenase regulates RANKL-mediated osteoclastogenesis via AMPK/c-Fos/NFATc1 signaling. *Biochem. Biophys. Res. Commun.* 475, 125–132. <https://doi.org/10.1016/j.bbrc.2016.05.055>.
 27. Ye, J., Gu, Y., Zhang, F., Zhao, Y., Yuan, Y., Hao, Z., Sheng, Y., Li, W.Y., Wakeham, A., Cairns, R.A., and Mak, T.W. (2017). IDH1 deficiency attenuates gluconeogenesis in mouse liver by impairing amino acid utilization. *Proc. Natl. Acad. Sci. USA* 114, 292–297. <https://doi.org/10.1073/pnas.1618605114>.
 28. Wang, M., Zhou, C., Yu, L., Kong, D., Ma, W., Lv, B., Wang, Y., Wu, W., Zhou, M., and Cui, G. (2022). Upregulation of MDH1 acetylation by HDAC6 inhibition protects against oxidative stress-derived neuronal apoptosis following intracerebral hemorrhage. *Cell. Mol. Life Sci.* 79, 356. <https://doi.org/10.1007/s00018-022-04341-y>.
 29. Nazio, F., Strappazon, F., Antonioli, M., Bielli, P., Cianfanelli, V., Bordi, M., Gretzmeier, C., Dengjel, J., Piacentini, M., Fimia, G.M., and Cecconi, F. (2013). mTOR inhibits autophagy by controlling ULK1 ubiquitylation, self-association and function through AMBRA1 and TRAF6. *Nat. Cell Biol.* 15, 406–416. <https://doi.org/10.1038/ncb2708>.
 30. Kim, J.H., Seo, D., Kim, S.J., Choi, D.W., Park, J.S., Ha, J., Choi, J., Lee, J.H., Jung, S.M., Seo, K.W., et al. (2018). The deubiquitinating enzyme USP20 stabilizes ULK1 and promotes autophagy initiation. *EMBO Rep.* 19, e44378. <https://doi.org/10.15252/embr.201744378>.
 31. Broeks, M.H., Shamseldin, H.E., Alhashem, A., Hashem, M., Abdulwahab, F., Alshedi, T., Alobaid, I., Zwartkruis, F., Westland, D., Fuchs, S., et al. (2019). MDH1 deficiency is a metabolic disorder of the malate-aspartate shuttle associated with early onset severe encephalopathy. *Hum. Genet.* 138, 1247–1257. <https://doi.org/10.1007/s00439-019-02063-z>.
 32. Lee, S.M., Kim, J.H., Cho, E.J., and Youn, H.D. (2009). A nucleocytoplasmic malate dehydrogenase regulates p53 transcriptional activity in response to metabolic stress. *Cell Death Differ.* 16, 738–748. <https://doi.org/10.1038/cdd.2009.5>.
 33. Chen, L., Xiang, B., Wang, X., and Xiang, C. (2017). Exosomes derived from human menstrual blood-derived stem cells alleviate fulminant hepatic failure. *Stem Cell Res. Ther.* 8, 9. <https://doi.org/10.1186/s13287-016-0453-6>.
 34. Chen, Q., Wang, Y., Jiao, F., Cao, P., Shi, C., Pei, M., Wang, L., and Gong, Z. (2021). HDAC6 inhibitor ACY1215 inhibits the activation of NLRP3 inflammasome in acute liver failure by regulating the ATM/F-actin signalling pathway. *J. Cell Mol. Med.* 25, 7218–7228. <https://doi.org/10.1111/jcmm.16751>.
 35. Wang, Y., Chen, Q., Jiao, F., Shi, C., Pei, M., Wang, L., and Gong, Z. (2021a). Histone deacetylase 2 regulates ULK1 mediated pyroptosis during acute liver failure by the K68 acetylation site. *Cell Death Dis.* 12, 55. <https://doi.org/10.1038/s41419-020-03317-9>.

STAR★METHODS

KEY RESOURCES TABLE

REAGENT or RESOURCE	SOURCE	IDENTIFIER
Antibodies		
IDH1	Proteintech	Cat#: 12332-1-AP; RRID: AB_2123159
MDH1	Proteintech	Cat#: 15904-1-AP; RRID: AB_2143279
GAPDH	Proteintech	Cat#: 60004-1-Ig; RRID: AB_2107436
β-actin	Proteintech	Cat#: 20536-1-AP; RRID: AB_10700003
Acetylated lysine	Cell Signaling Technology	Cat#: 9441; RRID: AB_331805
Bacterial and virus strains		
MDH1 K118R AAV	Genomeditech	N/A
IDH1 K93R AAV	Genomeditech	N/A
Biological samples		
Normal donor and ALF patient liver tissues	Liver Transplantation Center of Zhongnan Hospital of Wuhan University	N/A
Chemicals, peptides, and recombinant proteins		
Fetal bovine serum	Gibco	Cat#: A5669701
DMEM/F12 medium	Gibco	Cat#: 11320033
DMEM medium	Gibco	Cat#: 11965092
D-galactosamine	Sigma–Aldrich	Cat#: G0500
Lipopolysaccharide	Sigma–Aldrich	Cat#: L2880
ACY1215	MCE	Cat#: HY-16026
MDH1 K107R, K118R, K239R, K298R plasmids	Genomeditech	Described in current manuscript
IDH1 K81R, K93R, K224R, K233R, K321R plasmids	Genomeditech	Described in current manuscript
Lipofectamine 2000	Invitrogen	Cat#: 11668019
MDH1 siRNA	RiboBio	N/A
IDH1 siRNA	RiboBio	N/A
Critical commercial assays		
IDH activity assay kit	Sigma–Aldrich	Cat#: MAK062
MDH activity assay kit	Sigma–Aldrich	Cat#: MAK196
Deposited data		
Raw data	Mendeley Data	https://data.mendeley.com/preview/h5vtjcrjnw?a=04660a54-68ee-4bbb-bf20-c52c3e230b1a
Experimental models: Cell lines		
AML-12	Pinuofei Biological	RRID: CVCL_0140
293T	Cell Collection Center of Wuhan University	RRID: CVCL_0063
Experimental models: Organisms/strains		
C57BL/6 mice	Experimental Animal Center of Wuhan University	N/A
Software and algorithms		
SPSS	IBM	Version 25.0
GraphPad Prism	GraphPad	Version 8.0
R Studio	R project	Version 4.1.1

RESOURCE AVAILABILITY

Lead contact

Further information and requests for resources should be directed to the lead contact, Zuojiang Gong (zjgong@163.com).

Materials availability

This study did not generate new unique reagents.

Data and code availability

- The data reported in this paper have been deposited at Mendeley Data and are publicly available as of the date of publication. Accession numbers are listed in the [key resources table](#).
- This paper does not report original code.
- The additional information required to reanalyze the data reported in this paper is available from the [lead contact](#) upon request.

EXPERIMENTAL MODEL AND SUBJECT DETAILS

Cell culture and treatment

The mouse liver cell line AML-12 (RRID: CVCL_0140) was obtained from Wuhan Pinuofei Biological Co. Ltd, which was grown in DMEM/F12 supplemented with 10% FBS. LPS (100 ng/mL) combined with D-Gal (44 $\mu\text{g/mL}$)³³ was used to stimulate cells except for those in the control group. ACY1215 (2.5 μM) was added 2 h in advance of LPS/D-Gal.³⁴ The cells were harvested 24 h after LPS/D-Gal administration. FBS and DMEM/F12 media were obtained from Gibco (USA). D-Gal and LPS were purchased from Sigma–Aldrich (USA). ACY1215 was purchased from MedChemExpress (USA). IDH1, MDH1, GAPDH and β -actin specific antibodies were obtained from Proteintech (China). Acetylated lysine (Ac-Lys) antibody was purchased from Cell Signaling Technology (USA).

Animal groups

Sixty-six male C57BL/6 mice (6–8 weeks, 20–25 g) were purchased from the Experimental Animal Center of Wuhan University. MDH1-K118R and IDH1-K93R AAVs were constructed to transfect the mice (AAV8, Genomeditech, China). The mice were acclimated for 5 days and then randomly divided into eleven groups: empty vector (EV) group, wild-type (WT) group, MDH1-K118R group, IDH1-K93R group, control group, LPS/D-Gal group, LPS/D-Gal + MDH1-K118R group, LPS/D-Gal + IDH1-K93R group, LPS/D-Gal + ACY1215 group, LPS/D-Gal + ACY1215 + MDH1-K118R group, and LPS/D-Gal + ACY1215 + IDH1-K93R group. Except for those in the EV, WT, MDH1-K118R, IDH1-K93R and control groups, the other mice were intraperitoneally injected with LPS (100 $\mu\text{g/kg}$) and D-Gal (400 mg/kg).³⁴ AAV was administered via tail vein injection at a dose of 1×10^{11} vg 4 weeks before LPS/D-Gal injection. ACY1215 (25 mg/kg) was administered by intraperitoneal injection 2 h before LPS/D-Gal injection.³⁴ At 24 h after LPS/D-Gal injection, the mice were sacrificed. The livers and serum were collected for experiments. The animal experiments were carried out in compliance with ARRIVE guidelines and other relevant regulations. Approval was granted by the Institutional Animal Care and Use Committee of Renmin Hospital of Wuhan University.

Clinical specimen collection

All human experiments were conducted in compliance with the relevant principles. Normal donor and ALF patient liver tissues were provided by the Liver Transplantation Center of Zhongnan Hospital of Wuhan University. The human studies were performed according to the principles of the Declaration of Helsinki. Approval was granted by the Ethics Committee of Renmin Hospital of Wuhan University. Informed consent was obtained from all individual participants included in the study.

METHOD DETAILS

siRNA transfection

AML-12 cells were seeded in 6-well plates at a density of 5×10^4 cells/well and grown to 70% confluence. The cells were divided into the NC group, LPS/D-Gal group, LPS/D-Gal + ACY1215 group, LPS/D-Gal + MDH1-siRNA or IDH1-siRNA group, and LPS/D-Gal + ACY1215 + MDH1-siRNA or IDH1-siRNA group. LPS/D-Gal was used to stimulate the cells except those in the NC group. MDH1-siRNA or IDH1-siRNA (RiboBio) transfection was performed 24 h prior to LPS/D-Gal stimulation and ACY1215 was added to the medium 2 h prior to LPS/D-Gal stimulation. The cells were harvested 24 h after LPS/D-Gal administration. Transfection was performed using Lipofectamine 2000 (Invitrogen, USA) according to the manufacturer's instructions.

Plasmid transfection

K107R, K118R, K239R, and K298R of MDH1 mutants (which carries a CMV promoter with an HA tag) and K81R, K93R, K224R, K233R, and K321R of IDH1 mutants (which carries a CMV promoter with a 3*FLAG tag) were constructed by Genomeditech (China). 293T cells (Cell Collection Center of Wuhan University, China, RRID: CVCL_0063) were seeded into 6-well plates and transfected with plasmids mixed with Lipofectamine

2000 according to the manufacturer's instructions. For AML-12 cells, LPS/D-Gal and ACY1215 were used to stimulate the cells after plasmid transfection as described above.

Detection of energy metabolites

Energy metabolites were detected by liquid chromatography-mass spectrometry/mass spectrometry (LC-MS/MS). The experimental procedures were performed as follows: metabolite extraction, quality control preparation, sample LC-MS/MS analysis, data processing, and quantitative analysis. Specifically, proteins in the sample were precipitated with methanol/acetonitrile (1:1). After centrifugation, the supernatant was collected and added to an equal amount of the internal standard L-glutamate-d5 for vacuum drying. Acetonitrile/water (1:1) was used to redissolve the samples. After centrifugation, the supernatant was collected for analysis. A Shimadzu Nexera X2 LC-30AD high-performance liquid chromatograph was used for separation. A QTRAP5500 mass spectrometer (AB SCIEX) was used for mass spectrometry in positive/negative ion mode.

Immunofluorescence (IF)

The IF experiment was performed as previously reported.³⁴ After being treated, the cells were fixed with 4% paraformaldehyde, permeabilized with 0.2% Triton, blocked with 5% bovine serum albumin (BSA), and incubated with primary antibodies (1:100) overnight and secondary antibodies (Servicebio, China) for 1 h. The results were observed under a fluorescence microscope (Olympus, Japan).

Western blotting and immunoprecipitation (IP)

IP with antibodies and the subsequent western analyses were done as previously reported.¹⁹ The samples were lysed in radioimmunoprecipitation assay (RIPA) buffer and then centrifuged. Loading buffer was added, and the samples were boiled and analyzed by western blotting. Sodium dodecyl sulfate-polyacrylamide gel electrophoresis (SDS-PAGE) was used to separate the proteins. After electrophoresis, the proteins were transferred to a polyvinylidene fluoride (PVDF) membrane (Millipore, USA) and then the membrane was cropped and incubated with specific primary antibodies (1:1000 dilution except GAPDH and β -actin, which were 1:2000) and secondary antibodies (Cell Signaling Technology, USA). GAPDH or β -actin was used as a loading control. The results were detected by an Odyssey infrared imaging system.

The samples were lysed (500 μ L of IP buffer in a 10-centimetre Petri dish), incubated (5 μ g of primary antibodies or IgG), incubated (30 μ L of protein A + G agarose), washed (IP buffer), resuspended (40 μ L of 1.5 \times loading buffer), boiled, and centrifuged. The supernatants were collected for western blot analysis.

Detection of the activities of MDH1 and IDH1

The activities of MDH1 and IDH1 were detected as previously reported.¹⁹ Proteins were immunoprecipitated by beads and eluted using acid eluent (after elution, neutralized with neutral eluent). MDH1 or IDH1 levels were normalized. IDH1 and MDH1 enzyme activity was evaluated by IDH (Cat No.: MAK062) and MDH (Cat No.: MAK196) activity assay kit (Sigma-Aldrich, USA). The experiments were performed according to the manufacturer's instructions. The change in absorbance at 450 nm was measured using a microplate reader (PerkinElmer, USA).

Hematoxylin-eosin (HE) staining and immunohistochemistry (IHC)

The HE and IHC experiments were performed as previously reported.³⁵ Briefly, fresh tissues were fixed with 4% paraformaldehyde, embedded in paraffin, processed for sectioning and stained with haematoxylineosin. For IHC, the slices were treated as follows: blocked (3% H₂O₂, 5 min), washed (phosphate buffer saline), incubated (corresponding buffer solution, 10 min), washed, blocked (5% BSA, 30 min), incubated with primary antibodies, washed, and incubated (secondary antibody). The results were analyzed under a microscope.

Detection of ALT, AST and TBIL

Alanine aminotransferase (ALT), aspartate aminotransferase (AST), and total bilirubin (TBIL) levels in mouse serum were tested by a fully automatic biochemical analyzer (ADVIA 2400, Siemens AG).

QUANTIFICATION AND STATISTICAL ANALYSIS

All data were analyzed using SPSS 25.0. GraphPad Prism 8.0 and R 4.1.1 software were used to generate the figures. The results are presented as mean \pm SD. Analysis of variance (ANOVA) followed by a post-test (least significant difference test for homogeneity of variance; the Tamhane test for heterogeneity of variance) was used to analyze the differences between groups. $p < 0.05$ was considered statistically significant.